Published in final edited form as:
Int J Cancer. 2004 July 20; 110(6): 800–806. doi:10.1002/ijc.20206.

PROGRESSION TO ANDROGEN-INDEPENDENT LNCAP HUMAN PROSTATE TUMORS: CELLULAR AND MOLECULAR ALTERATIONS

Jin-Rong ZHOU[1,*], **Lunyin YU**[1], **Luiz F. ZERBINI**[2], **Towia A. LIBERMANN**[2], and **George L. BLACKBURN**[1]

1*Nutrition/Metabolism Laboratory, Department of Surgery, Beth Israel Deaconess Medical Center, Harvard Medical School, Boston, MA, USA*

2*New England Baptist Bone & Joint Institute, The Genomics Center, Beth Israel Deaconess Medical Center, Harvard Medical School, Boston, MA, USA*

Abstract

Lethal phenotypes of human prostate cancer are characterized by progression to androgen-independence and metastasis. For want of a clinically relevant animal model, mechanisms behind this progression remain unclear. Our study used an *in vivo* model of androgen-sensitive LNCaP human prostate cancer cell xenografts in male SCID mice to study the cellular and molecular biology of tumor progression. Primary tumors were established orthotopically, and the mice were then surgically castrated to withdraw androgens. Five generations of androgen-independent tumors were developed using castrated host mice. Tumor samples were used to determine expressions of cellular and molecular markers. Androgen-independent tumors had increased proliferation and decreased apoptosis compared to androgen-sensitive tumors, outcomes associated with elevated expression of p53, p21/waf1, bcl-2, bax and the bcl-2/bax ratio. Blood vessel growth in androgen-independent tumor was associated with increased expression of vascular endothelial growth factor. Overexpression of androgen receptor mRNA and reduced expression of androgen receptor protein in androgen-independent tumors suggest that the androgen receptor signaling pathway may play an important role in the progression of human prostate cancer to androgen-independence. The *in vivo* orthotopic LNCaP tumor model described in our study mimics the clinical course of human prostate cancer progression. As such, it can be used as a model for defining the molecular mechanisms of prostate cancer progression to androgen-independence and for evaluating the effect of preventive or therapeutic regimens for androgen-independent human prostate cancer.

Keywords

prostate cancer; *androgen-sensitive*; *androgen-independent*; *orthotopic model*

Prostate carcinoma is the second leading cause of cancer death in American men, with 1 in every 5 patients developing invasive cancer. It accounts for an estimated 29% of all new cancer cases diagnosed in U.S. men.[1] Most prostate cancer is initially androgen-dependent (AD). In 80% of men who receive androgen blockade therapy, cancer cells die and patients show improvement. In time, however, nearly all tumors grow back to androgen-independence (AI).

*Correspondence to: Nutrition/Metabolism Laboratory, Department of Surgery, Beth Israel Deaconess Medical Center, Harvard Medical School, 330 Brookline Avenue, Burlington-554B, Boston, MA 02215. Fax: +617-632-0275. E-mail: E-mail: jrzhou@bidmc.harvard.edu.

Clinically, the lethal phenotypes of human prostate cancer are characterized by progression to androgen-independence.[2]

The search for effective therapies for prostate cancer and in particular for ways to intervene in the progression of AI tumors has been hampered by a lack of clinically relevant animal models. The ability to validate new concepts requires representative model systems of human origin that mimic the clinical process of the disease in patients. In some animal models, prostate tumors have been developed and progressed subcutaneously, therefore tumor-host interactions in these models are different from that in humans. Coinoculation of tumor cells with specific fibroblasts (*e.g.* prostate and bone fibroblasts) has improved tumor cell-host cell interaction.[3,4] An *in vivo* orthotopic prostate tumor model, which mirrors tumor cell-host interactions in humans, is considered even more relevant.[5,6]

Our understanding of the mechanisms of progression of AD prostate cancer to AI prostate cancer has been largely obtained through the study of experimental animal models. The cellular and molecular responses of AD tumors to androgen ablation have been described in studies using *in vivo* animal models that mimic the progression of prostate cancer after surgical castration.[4,7-9] Previous animal studies have produced inconsistent and contradictory findings on the effects of androgen withdrawal on tumor AR expression,[4,8,10-14] apoptosis[7-9] and proliferation.[7-9] These results suggest that tumor cell biology as well as nonandrogenic variables (*e.g.*, extracellular matrix pathways or altered growth factors) may play roles in the regulation of prostate cancer progression and the modulation of cellular and molecular events.[3,4,15]

In our study, we developed an *in vivo* animal model of human prostate cancer progression from androgen-sensitive (AS) to AI by surgical castration of SCID mice bearing orthotopic LNCaP human prostate tumor. This *in vivo* androgen-sensitive prostate tumor model resembles tumor-stromal interactive microenvironments in humans. To investigate the effects of androgen withdrawal on cellular and molecular markers, we grew 5 generations of AI tumors in castrated host animals. We established that this *in vivo* orthotopic model of AI tumor progression has clinical relevance in the evaluation of preventive or therapeutic regimens for AI human prostate cancer.

MATERIAL AND METHODS

Orthotopic implantation of LNCaP tumor cells

Eight-week-old male SCID beige mice were purchased from Taconic (Germantown, NY) and housed in a pathogen-free environment. Immediately before implantation, exponentially growing LNCaP cells were trypsinized and resuspended in DMEM with 10% FBS, cell viability was determined by Trypan blue exclusion, and a single-cell suspension with >90% viability was used for implantation. A transverse incision was made in the lower abdomen, and the bladder and seminal vesicles were delivered through the incision to expose the dorsal prostate. LNCaP cells (2×10^6 cells in 50 μL medium) were carefully injected under the prostatic capsule via a 30-gauge needle. Proper inoculation of cell suspension was indicated by blebbing under the prostatic capsule. The incision was closed using a running suture of 5-0 silk. All procedures with animals were reviewed and approved by the Institutional Animal Care and Use Committee at Beth Israel Deaconess Medical Center according to the NIH guidelines.

Establishment and passage of AI prostate cancer

When the AS tumor was developed, androgen withdrawal was accomplished by surgical castration. The AS tumor regressed initially in response to androgen ablation and then regrew to develop the AI tumor (the first generation, abbreviated as AI-1), as monitored by increase

of serum prostate-specific antigen (PSA) and tumor volume. The AI-1 tumor was then orthotopically implanted into castrated SCID host mice to develop the second generation of the AI tumor (AI-2). This process was repeated 3 more times so that the third (AI-3), the forth (AI-4) and the fifth (AI-5) generation of AI tumor sublines were developed. Biologic samples from at least 4 mice in each generation were collected for analysis.

Tumor histology

For histologic examination, tumor tissues were fixed in 10% buffered neutralized formalin, embedded in paraffin, cut into 5 μm sectiona and stained with hematoxylin-eosin.

In situ *detection of apoptotic index*

Apoptotic cells were determined by a terminal deoxynucleotidyl transferase-mediated dUTP-biotin nick end labeling (TUNEL) assay using the ApopTag plus peroxidase *in situ* apoptosis detection kit (Intergen, Purchase, NY) according to our previous procedures.[6,16] Six representative areas of each section without necrosis were selected, and both apoptotic cells and total nuclei cells were counted under a light microscope at 400× magnification. The apoptotic index was expressed as the percentage of positive apoptotic tumor cells to total tumor cells.

Tumor blood vessel

Six nonnecrotic and nonblooded fields in each H&E-stained tumor specimen were selected, and visible blood vessels within the same area were counted under microscope at 200× magnification.

Immunohistochemical determinations of AR, p53, p21/wafl and Ki-67

Automated immunohistochemistry followed by image analysis was applied to quantify the expression of AR, p53, p21/wafl and Ki-67, according to our previously described procedures.[6] In brief, after deparaffinization, rehydration and washing, the section was soaked in 10 mM citrate buffer (pH 6.0) and heated for 20 min in a microwave oven. After being cooled to room temperature, the section was treated with 1% hydrogen peroxide for 5 min, then stained by using an automated staining machine (ES; Ventana Medical Systems, Tucson, AZ). The section was incubated with the primary antibody for 32 min and incubated with a biotinylated universal anti-mouse/rabbit IgG (VECTASTAIN, 1:100 dilution). The section was then stained with 3-3′ diaminobenzidine and counterstained with hematoxylin and a bluing agent by using 3-3′ diaminobenzidine Detection Kit (Ventana Medical Systems). Digital images of 5 fields in each tissue section were acquired at 400× magnification with a digital camera (CoolSNAP; RS Photometrics, Tucson, AZ) mounted on a light microscope (Leica DMLS; Leica Microsystems Wetzlar, Ernst-Leitz-Strasse, Germany). True-color image analysis was performed by using IPLab 3.5 image analysis software (Scanalytics, Fairfax, VA) to quantify the percentages of positive tumor cells to total tumor cells. Both positive- and negative-control slides were used to confirm the sensitivity and specificity of staining. The antibodies and dilutions were as follows: a mouse anti-human AR monoclonal antibody (1:50, Clone AR441, DAKO, Carpinteria, CA), a mouse anti-human p53 monoclonal antibody (1:100, DO-1, reactive with both wild and mutant p53; Santa Cruz Biotechnology, Santa Cruz, CA), a mouse anti-human p53 monoclonal antibody (1:25, Pab 240, reactive with mutant p53 only, Santa Cruz Biotechnology), a mouse anti-human p21/wafl monoclonal antibody (1:100, AB-1; Calbiochem, San Diego, CA), a mouse anti-human Ki-67 monoclonal antibody (1:20, Ki-S5; DAKO).

Immunohistochemical determination of proliferation index

Ki-67 was determined by immunohistochemical staining to quantify the proliferation index, as described above. Both Ki67-positive proliferating cells and total tumor cells were counted in 3 nonnecrotic areas of each section using light microscopy at 400× magnification. The proliferation index was calculated as the percentage of Ki-67-positive tumor cells to total tumor cells.

Western blot analysis

Western blot analysis was performed to determine the expression of bcl-2, bax and vascular endothelial growth factor (VEGF). The housekeeping protein GAPDH was used as the control. Total tumor cell lysate was prepared by extracting total cellular proteins with lysis buffer [PBS, pH 7.4, 1% NP-40, 0.5% sodium deoxycholate, 0.1% SDS] and with freshly added proteinase inhibitors [10 mM N-ethylmaleimide, 10 μg/mL aprotinin, 2 μg/mL pepstatin A, 10 μg/mL leupeptin, 2 mM phenylmethylsulfonyl fluoride, 1.0 mM $NaVO_4$, 10 mM NaF], followed by centrifugation. Western blotting was performed based on standard procedures. In brief, proteins (50 μg) were separated by SDS-polyacrylamide gel and transferred onto polyvinylidene difluoride membrane. After blocking nonspecific sites by 5% milk overnight (nonfat dry milk in PBS), the membrane was incubated with primary antibodies for 60 min, washed and incubated with horseradish peroxidase-conjugated secondary antibody (1:2,000; Amersham Life Science, Arlington Heights, IL). Primary antibodies used for Western blot analysis were anti-Bcl-2 monoclonal (1:50, clone 124; DAKO), anti-bax monoclonal (1:50, AB-1; Oncogene), anti-VEGF monoclonal (2.5 μg/ml AB-2; Oncogene) and anti-GAPDH monoclonal (0.1 μg/ml, Clone 6C5; Research Diagnostics, Flanders, NJ). Western blots were developed using the chemiluminescent reagent (ECL; Amersham Life Science) according to the manufacturer's instructions. The levels of protein expression were quantified by densitometry using Bio-Rad GS-700 Imaging Densitometer (Bio-Rad Laboratory, Hercules, CA) and NIH image analysis program (NIH Image 1.62).

Reverse transcription-PCR (RT-PCR)

AR mRNA was determined by RT-PCR. Total RNA was extracted from tumor tissues using the RNeasy Mini Kit (Qiagen, Valencia, CA) according to the manufacturer's protocol. cDNA was prepared using Ready-To-Go, You-Prime First-Strand Beads (Amersham Pharmacia, Piscataway, NJ). The primer pairs for AR (5′-AGA TGG GCT TGA CTT TCC CAG AAA G-3′ and 5′-ATG GCT GTC ATT CAG TAC TCC TGG A-3′) and for GAPDH (5′-CAAAGT TGT CAT GGA TGA CC-3′ and 5′-CCA TGG AGA AGG CTG GGG-3′) were purchased for PCR from Invitrogen Life Technologies (Frederick, MD). PCR was performed according to standard procedures by using Eppendorf Mastercycler (Eppendorf Scientific, Westbury, New York). Thermal cycling was performed by initial denaturation at 94°C for 2 min, followed by 40 cycles according to the following cycle profile: denaturation at 94°C for 45 sec, annealing at 50°C for 45 sec and elongation at 72°C for 1 min. After PCR, electrophoresis was run to ensure that a right-size product was amplified in the reaction by using Tris/EDTA (TAE)-buffered agarose gels (1.5%). NIH Image 1.62 software was used to quantify the expression of AR mRNA.

Statistical analysis

All data were expressed as group means ± SEM. Data were analyzed by analysis of variance followed by Fisher's protected least-significant difference[17] using Statview 5.0 program (SAS Institute, Cary, NC). A p-value < 0.05 was considered as statistically significant.

RESULTS

Effects of AI tumor progression on tumor growth, metastasis and histology

We have developed an *in vivo* model of AI prostate cancer from AS prostate cancer by using intraprostatic inoculation of LNCaP human prostate cancer cells in mice. Castration initially inhibited the orthotopic growth of LNCaP tumor and lowered serum PSA levels. Tumors then started to grow again in the absence of testicular androgen to develop the AI tumor. The time required for tumor to regrow to AI was dependent upon the size of AS tumor before castration. The AI tumor was then harvested and orthotopically implanted to the castrated host mouse to develop a total of 5 generations of the AI tumor. During development of the AI tumors, the rates of tumorigenicity were 100%. AI tumors grew faster with each generation. The average time required for AI-1 tumor development was about twice as that for AI-4 and AI-5 tumor development.

Serum level of PSA was measured by ELISA assay. AI tumors secreted PSA to blood, and PSA levels were associated with tumor size. Since tumors were not collected at the same size or the same time, the comparisons of serum PSA levels between different generations of tumors were less meaningful and thus were not performed. The metastasis rate was not evaluated because of the small number of samples ($n = 4$ for each group).

Effects of AI tumor progression on AR expression

The effects of androgen withdrawal on the expression of AR transcript and protein were determined by RT-PCR and immunohistochemistry, respectively. Compared to the AS tumors (Fig. 1*a*), the AI tumors had reduced expression of AR protein (Fig. 1*b*). Almost all of the AS tumor cells (92.6%) were AR-positive. But the percentages of AR-positive cells in different generations of AI tumors were gradually reduced from 83.3% ($p < 0.05$), 76.2% ($p < 0.01$), 59.1% ($p < 0.01$), 63.6 % ($p < 0.01$) to 59.2% ($p < 0.01$) (Fig. 1*c*).

In contrast to AR protein expression, RT-PCR analysis indicated that the AI tumors had increased expression of AR mRNA compared to the AS tumor (Fig. 1*d*). There were no differences of AR mRNA expressions between AI tumors. Image analysis showed that the AR mRNA expressions in the AI tumors were twice as that in the AS tumors ($p < 0.05$).

Effects of AI tumor progression on cell proliferation

Ki-67 staining was used to determine the prostate cancer cell proliferation index. The AI tumor progression significantly increased tumor cell proliferation. The proliferation indices in the AI-1, AI-2, AI-3, AI-4 and AI-5 tumor cells were increased by 122% ($p < 0.05$), 133.5% ($p < 0.05$), 139.0% ($p < 0.05$), 122.6% ($p < 0.05$) and 123.8% ($p < 0.05$), respectively, compared to that of the AS tumor (Table I). There were no further significant changes of cell proliferation among AI tumors (Table I).

Effects of AI tumor progression on apoptosis and the expression of apoptosis modulators

The TUNEL assay was used to determine the *in situ* apoptosis of prostate tumor cells. The apoptotic index in the AI-1 tumor was significantly inhibited by 72% ($p < 0.01$), and there were no further significant changes of apoptosis in subsequent AI tumors (Table I).

The expressions of the apoptosis promoters p53, p21/wafl and Bax and the apoptosis inhibitor bcl-2 in tumors were detected by immunohistochemistry or Western blot to further elucidate the molecular mechanisms by which the development of AI prostate cancer modulates tumor cell apoptosis. The p53-positive cells in the AI-1, AI-2, AI-3, AI-4 and AI-5 tumors increased 39.7% ($p > 0.05$), 342.6% ($p < 0.01$), 301.5% ($p < 0.01$), 313.2% ($p < 0.01$) and 339.7% ($p < 0.01$), respectively, compared to the AS tumors (Table I). In addition to increased numbers of

p53-positive cells, the AI tumors also had significantly increased intensity of p53 expression in p53-positive cells by 30.5% to 53% ($p < 0.01$, Table I). Similar to p53, the p21/waf1-positive cells in the AI-1, AI-2, AI-3, AI-4 and AI-5 tumors increased by 310.5% ($p < 0.05$), 248.6% ($p > 0.05$), 449.9% ($p < 0.01$), 374.6% ($p < 0.05$) and 228.5% ($p > 0.05$), respectively (Table I). The intensities of p21/waf1 protein in p21/wafl-positive cells also significantly increased by 54.3% to 68.9% in the AI tumors ($p < 0.01$).

Both bcl-2 and bax proteins were significantly higher in the AI tumors than that in the AS tumors (Fig. 2*a*). The increase of bcl-2 expression was higher than that of Bax, resulting in significant 3-7-fold increases of bcl-2/Bax ratios in the AI tumors (Fig. 2*b*).

Effects of AI tumor progression on blood vessel formation and the expression of angiogenic factor VEGF

The number of blood vessels in tumors were counted in H&E-stained slides. The AI tumor showed more blood vessels than the AS tumor (Fig. 3*a*). Compared to that of the AS tumor, the blood vessel numbers in the AI-1, AI-2, AI-3, AI-4 and AI-5 tumors were significantly increased by 129% ($p < 0.01$), 200% ($p < 0.01$), 213% ($p < 0.01$), 367% ($p < 0.01$) and 288% ($p < 0.01$), respectively. In parallel, Western blot analysis indicated that the AI tumor progression significantly increased VEGF expression by 0.5-3-fold in the AI tumors, compared to that in the AS tumors (Fig. 3*b*,*c*).

DISCUSSION

In our study, we used an orthotopic animal model of AS human LNCaP prostate cancer progression to mimic the tumor cell-host cell interactive microenvironments and evaluate cellular and molecular changes during AI tumor progression. We also grew orthotopic AI tumors in up to 5 generations of castrated host animals. Progression to androgen independence was associated with increased proliferation and reduced apoptosis of prostate cancer cells. We also determined mRNA and protein expression of AR using RT-PCR and immunohistochemistry, respectively. Results (Fig. 1*d*) showed a 2-fold increase in expression of AR mRNA in all 5 generations of AI tumors and a gradual decline in expression of AR protein, by 10% from the AI-1 tumor to 36% by the AI-5 tumor. These findings indicate that androgen withdrawal may have the opposite effect on AR transcription and translational or posttranslational modification processes, and AI progression is associated with a reduction of AR function.

To be clinically relevant, animal models must meet certain strict criteria, *i.e.*, tumor cell maintenance of key biologic traits of the human prostate, such as secretion of PSA; sensitivity to or dependence on androgen for growth; AI tumor development from an AD carcinoma after androgen withdrawal; and growth of primary tumor cells in the relevant environment. Thalman *et al.* found that unlike other human prostate cancer models, the LNCaP progression model shares remarkable similarities with human prostate cancer.[2] Orthotopic LNCaP tumor model mirrors tumor cell-host interactions in humans and is considered more clinically relevant.[5,6] This orthotopic SCID-LNCaP tumor model was used in our study to determine the alterations of tumor markers associated with progression of AI prostate tumors after androgen ablation treatment, therefore the results were expected to be significant clinically.

The molecular mechanisms that underlie the transition of prostate tumors from AS to AI status remain unknown. Evidence suggests that the AR signaling pathway could play a central role.[18] AR expression occurred in both kinds of tumors,[19,20] but the levels of expression were found to vary. Some studies reported increased expression of AR in hormone-refractory AI tumors;[10-13,21,22] others, however, found decreased expression of AR in AI tumors.[14,19,23,24] In reviewing the literature, we found that the studies reporting increased expression of

AR were those determining AR mRNA expressions, and that the studies reporting decreased expression of AR were those determining AR protein expression. Unfortunately, previous research measured either mRNA or AR protein. In our study, we determined both mRNA and protein expression of AR. Results showed that AR mRNA expression was increased 2-fold in all 5 generations of AI tumors, whereas AR protein expression was decreased gradually from the AI-1 tumor to the AI-5 tumor (Fig. 1*c*,*d*). Our results provide evidence to understand the nature of AR modulation by androgen ablation in prostate cancer progression. Our results, together with others, suggest that AI tumor progression due to androgen ablation is associated with increased AR transcript but with decreased AR protein. Additional studies on how androgen ablation alters AR transcription and translation may further elucidate the tumor progression process and facilitate the development of novel therapies.

Clinical progression of prostate cancer after hormonal therapy is usually associated with reduced apoptosis and increased proliferation of prostate cancer cells. Androgen ablation treatment induced initial apoptosis in AD prostate cancer.[25] Progression of AI tumors was associated with significant reductions in apoptosis and nonsignificant increases (23%) in proliferation compared to AD tumors[26,27] and that the low apoptotic index in primary prostate tumor was associated with poor response to hormonal therapy.[27] Conversely, findings from animal studies are inconsistent. Bladou *et al.*[9] found a decrease in the proliferation index after castration and progression of the AI tumor; a significant drop in tumor growth rate, followed by an increase; and an initial rise in the apoptotic index, followed by a decline; the AI tumor relapse after castration was associated with a reduced apoptosis with no increase in proliferation.[9] Landstrom *et al.*[7] reported an association between regrowth of AI prostate tumors and a reduction in apoptosis; AI tumor regrowth was not, however, associated with increased cell proliferation. Agus *et al.*[8] found that androgen withdrawal produced an initial decrease in prostate cancer cell proliferation, followed by increases consistent with AI tumor regrowth; apoptosis remained unchanged during regression and regrowth. Therefore, more studies are needed by using clinically relevant animal models to characterize alterations of tumor markers associated with androgen ablation and progression to AI tumors.

Our study describes an association between regrowth of AI tumors and both decreased apoptosis and increased proliferation of tumor cells. Results (Table I) also showed maintenance of apoptosis and proliferation rates from the first to the fifth generations of AI tumors. These results, which are consistent with clinical findings,[26,27] suggest that our animal model for orthotopic AI tumor progression could provide a clinically relevant *in vivo* model of AI tumor progression for studies of apoptosis and proliferation mechanisms.

Molecular mechanisms behind the modulation of tumor apoptosis and proliferation by androgen withdrawal have been studied extensively. Apoptosis is a major physiologic means of cell removal, a process that involves many molecular modulators, such as bcl-2, bax, p53 and p21/WAF1. Proteins encoded by bcl-2 family genes are important regulators of apoptosis. Expression of bcl-2 tended to be more frequent in high-grade tumors and metastases than in lower-grade and nonmetastatic tumors.[28,29] Apoptosis resistance was associated with higher levels of bcl-2.[29,30] Overexpression of bcl-2 after androgen ablation was correlated with the progression of prostate cancer from androgen dependence to androgen independence.[31] These findings suggest that bcl-2 protein might be a factor that enables prostate cancer cells to survive in androgen-deprived environments. The tumor suppressor gene p53, known to be involved in the regulation of cell growth and apoptosis, was implicated in hormone refractory prostate cancer and poor prognosis. p53 protein accumulation and mutation were associated with increased cell proliferation rate, increased histologic grade and stage and transition from AD to AI growth.[32] Metastatic and hormone-refractory tumors showed increased p53 protein expression associated with p53 gene alterations.[33-35] Both bcl-2 and p53 protein accumulations were observed in hormone-refractory prostate cancer.[35] Clinically, patients

who showed overexpression of bcl-2 or p53 had a significantly higher 5-year failure rate than those who don't.[36]

Our study described increased expression of p53 (Table I) and bcl-2 proteins (Fig. 2) in AI tumors, findings consistent with clinical observations. It has been suggested that the bcl-2/bax ratio might be a better indicator of tumor apoptosis than p53 or bcl-2 protein accumulations.[37] In our study, we observed increased expression of both bcl-2 and bax. The rise in bcl-2 expression, however, was much higher than that in bax. In turn, bcl-2/bax ratios were 3- 6-fold higher in the different generations of AI tumors (Fig. 2). These results, which mirror clinical findings, suggest that our animal model of orthotopic AI tumor progression can be used as a clinically relevant *in vivo* model for investigation of the molecular mechanisms by which androgen ablation leads to progression of AI tumors.

Human prostate tumors are dependent on angiogenesis for growth, and VEGF is a major regulator of this process. Androgens upregulated VEGF expression, and hormone-ablation-induced tumor-growth inhibition was associated with a decrease in VEGF expression and markedly reduced tumor neovascularization.[38-40] However, relapse of prostate tumors after androgen-ablation therapy was associated with increased angiogenesis and VEGF expression.[41] By using an orthotopic prostate tumor model, we found that the progression of AI prostate tumor was associated with increased tumor vascularization and expression of VEGF. It suggests that our animal model of can be used as a clinically relevant *in vivo* model for investigation of the molecular mechanisms by which relapse of androgen ablation treatment leads to increased angiogenesis and VEGF expression and for evaluation the efficacy of the antiangiogenic therapy on progression of AI prostate tumor.

In our study, up to 5 generations of AI tumors were used to characterize the alteration of tumor markers associated with androgen ablation and progression of AI tumors. The comparison of biomarkers in different generations of tumors provided important information on understanding the long-term effects of androgen ablation treatment on tumor marker modulation. As our results show, both tumor cell proliferation and apoptosis indices, two primary parameters that are associated with development of androgen independence of prostate tumor, were significantly altered in AI-1 tumors compared to the AS tumors, and no further alterations were observed in other generations of AI tumors. AI-1 tumors also showed significantly more blood vessels than the AS tumors, although more blood vessels were present in the later generations of the AI tumors. This observation is consistent with the clinical observation that development of the AI tumor is associated with increased angiogenesis. Even though different molecular markers may have had slightly different time-dependent responses to androgen ablation, all markers showed similar trends of alteration among different AI tumors, suggesting that alterations of these molecular markers are consistent with that of the cellular markers. These results suggest that AI-1 tumor is sufficient to represent the androgen-independent prostate tumor.

In conclusion, hormone withdrawal-induced AI tumor progression was associated with increased proliferation and decreased apoptosis of prostate tumor cells, increased expressions of p53, bcl-2 and bcl-2/bax ratios, increased tumor vascularization and VEGF expression and the decreased AR protein/function. The *in vivo* orthotopic LNCaP tumor model described in our study mimics the clinical course of human prostate cancer. As such, it can be used as a model for defining the molecular mechanisms of prostate cancer progression and for evaluating the efficacy of treatment for AI/hormone-refractory prostate cancer.

ACKNOWLEDGEMENTS

This work was supported in part by Massachusetts Department of Public Health Prostate Cancer Research Program, RO3 CA 10104 (National Cancer Institute, NIH) and RO1 CA 78521 (National Cancer Institute, NIH) [to J-RZ] and by DAMD 170110023 (U.S. Army) and RO1 CA 85467 (National Cancer Institute, NIH) [to TAL].

Abbreviations

AD, androgen-dependent; AI, androgen-independent; AR, androgen receptor; AS, androgen-sensitive; PSA, prostate-specific antigen; TUNEL, terminal deoxynucleotidyl transferase-mediated dUTP-biotin nick end labeling; RT-PCR, reverse transcription-polymerase chain reaction; VEGF, vascular endothelial growth factor.

REFERENCES

1. Landis SH, Murray T, Bolden S, Wingo PA. Cancer Statistics. CA Cancer J Clin 1999;49:8–31. [PubMed: 10200775]
2. Thalmann GN, Sikes RA, Wu TT, Degeorges A, Chang SM, Ozen M, Pathak S, Chung LW. LNCaP progression model of human prostate cancer: androgen-independence and osseous metastasis. Prostate 2000;44:91–103. [PubMed: 10881018]
3. Gleave ME, Hsieh JT, Gao C, Chung LWK, von Eschenbach AC. Acceleration of human prostate cancer growth in vivo by prostate and bone fibroblasts. Cancer Res 1991;51:3753–61. [PubMed: 1712249]
4. Wu HC, Hsieh JT, Gleave ME, Brown NM, Pathak S, Chung LW. Derivation of androgen-independent human LNCaP prostatic cancer cell sublines: role of bone stromal cells. Int J Cancer 1994;57:406–12. [PubMed: 8169003]
5. Sato N, Gleave ME, Bruchovsky N, Rennie PS, Beraldi E, Sullivan LD. A metastatic and androgen-sensitive human prostate cancer model using intraprostatic inoculation of LNCaP cells in SCID mice. Cancer Res 1997;57:1584–9. [PubMed: 9108464]
6. Zhou J-R, Yu L, Zhong Y, Nassr RL, Franke AA, Gaston SM, Blackburn GL. Inhibition of orthotopic growth and metastasis of androgen-sensitive human prostate tumors in mice by bioactive soybean components. Prostate 2002;53:143–53. [PubMed: 12242729]
7. Landstrom M, Damber J-E, Bergh A. Prostatic tumor regrowth after initially successful castration therapy may be related to a decreased apoptotic cell death rate. Cancer Res 1994;54:4281–4. [PubMed: 7913874]
8. Agus DB, Cordon-Cardo C, Fox W, Drobnjak M, Koff A, Golde DW, Scher HI. Prostate cancer cell cycle regulators: response to androgen withdrawal and development of androgen independence. J Natl Cancer Inst 1999;91:1869–76. [PubMed: 10547394]
9. Bladou F, Vessella RL, Buhler KR, Ellis WJ, True LD, Lange PH. Cell proliferation and apoptosis during prostatic tumor xenograft involution and regrowth after castration. Int J Cancer 1996;67:785–90. [PubMed: 8824549]
10. Koivisto P, Kononen J, Palmberg C, Tammela T, Hyytinen E, Isola J, Trapman J, Cleutjens K, Noordzij A, Visakorpi T, Kallioniemi OP. Androgen receptor gene amplification: a possible molecular mechanism for androgen deprivation therapy failure in prostate cancer. Cancer Res 1997;57:314–9. [PubMed: 9000575]
11. Linja MJ, Savinainen KJ, Saramaki OR, Tammela TL, Vessella RL, Visakorpi T. Amplification and overexpression of androgen receptor gene in hormone-refractory prostate cancer. Cancer Res 2001;61:3550–5. [PubMed: 11325816]
12. Bubendorf L, Kononen J, Koivisto P, Schraml P, Moch H, Gasser TC, Willi N, Mihatsch MJ, Sauter G, Kallioniemi OP. Survey of gene amplifications during prostate cancer progression by high-throughout fluorescence in situ hybridization on tissue microarrays. Cancer Res 1999;59:803–6. [PubMed: 10029066]
13. Miyoshi Y, Uemura H, Fujinami K, Mikata K, Harada M, Kitamura H, Koizumi Y, Kubota Y. Fluorescence in situ hybridization evaluation of c-myc and androgen receptor gene amplification and

chromosomal anomalies in prostate cancer in Japanese patients. Prostate 2000;43:225–32. [PubMed: 10797498]

14. Kinoshita H, Shi Y, Sandefur C, Meisner LF, Chang C, Choon A, Reznikoff CR, Bova GS, Friedl A, Jarrard DF. Methylation of the androgen receptor minimal promoter silences transcription in human prostate cancer. Cancer Res 2000;60:3623–30. [PubMed: 10910077]
15. Chung LW, Li W, Gleave ME, Hsieh JT, Wu HC, Sikes RA, Zhau HE, Bandyk MG, Logothetis CJ, Rubin JS. Human prostate cancer model: roles of growth factors and extracellular matrices. J Cell Biochem Suppl 1992;16H:99–105. [PubMed: 1289680]
16. Zhou J-R, Gugger ET, Tanaka T, Guo Y, Blackburn GL, Clinton SK. Soybean phytochemicals inhibit the growth of transplantable human prostate carcinoma and tumor angiogenesis in mice. J Nutr 1999;129:1628–35. [PubMed: 10460196]
17. Steel, RGD.; Torrie, JH. Principles and procedures of statistics: a biometrical approach. Vol. 2nd ed. McGraw-Hill; New York: 1980.
18. Grossmann ME, Huang H, Tindall DJ. Androgen receptor signaling in androgen-refractory prostate cancer. J Natl Cancer Inst 2001;93:1687–97. [PubMed: 11717329]
19. Hobisch A, Culig Z, Radmayr C, Bartsch G, Klocker H, Hittmair A. Distant metastases from prostatic carcinoma express androgen receptor protein. Cancer Res 1995;55:3068–72. [PubMed: 7541709]
20. Hobisch A, Culig Z, Radmayr C, Bartsch G, Klocker H, Hittmair A. Androgen receptor status of lymph node metastases from prostate cancer. Prostate 1996;28:129–35. [PubMed: 8604394]
21. Visakorpi T, Hyytinen E, Koivisto P, Tanner M, Keinanen R, Palm-berg C, Palotie A, Tammela T, Isola J, Kallioniemi OP. In vivo amplification of the androgen receptor gene and progression of human prostate cancer. Nat Genet 1995;9:401–6. [PubMed: 7795646]
22. Taplin ME, Bubley GJ, Shuster TD, Frantz ME, Spooner AE, Ogata GK, Keer HN, Balk SP. Mutation of the androgen-receptor gene in metastatic androgen-independent prostate cancer. N Engl J Med 1995;332:1393–8. [PubMed: 7723794]
23. van der Kwast TH, Schalken J, Ruizeveld der Winter JA, van Vroonhoven CCJ, Mulder E, Boersma W, Trapman J. Androgen receptors in endocrine-therapy-resistant human prostate cancer. Int J Cancer 1991;48:189–93. [PubMed: 1708363]
24. Ruizeveld de Winter JA, Janssen PJ, Sleddens HM, Verleun-Mooijman MC, Trapman J, Brinkmann AO, Santerse AB, Schroder FH, van der Kwast TH. Androgen receptor status in localized and locally progressive hormone refractory human prostate cancer. Am J Pathol 1994;144:735–46. [PubMed: 7512791]
25. Montironi R, Magi-Galluzzi C, Fabris G. Apoptotic bodies in prostatic intraepithelial neoplasia and prostatic adenocarcinoma following total androgen ablation. Pathol Res Prac 1995;191:873–80.
26. Yang G, Wheeler TM, Kattan MW, Scardino PT, Thompson TC. Perineural invasion of prostate carcinoma cells is associated with reduced apoptotic index. Cancer 1996;78:1267–71. [PubMed: 8826950]
27. Palmberg C, Rantala I, Tammela TL, Helin H, Koivisto PA. Low apoptotic activity in primary prostate carcinomas without response to hormonal therapy. Oncol Rep 2000;7:1141–4. [PubMed: 10948353]
28. Krajewska M, Krajewski S, Epstein JI, Shabaik A, Sauvageot J, Song K, Kitada S, Reed JC. Immunohistochemical analysis of bcl-2, bax, bcl-X, and mcl-1 expression in prostate cancers. Am J Pathol 1996;148:1567–76. [PubMed: 8623925]
29. Raffo AJ, Perlman H, Chen MW, Day ML, Streitman JS, Buttyan R. Overexpression of bcl-2 protects prostate cancer cells from apoptosis in vitro and confers resistance to androgen depletion in vivo. Cancer Res 1995;55:4438–45. [PubMed: 7671257]
30. McConkey DJ, Greene G, Pettaway CA. Apoptosis resistance increases with metastatic potential in cells of the human LNCaP prostate carcinoma line. Cancer Res 1996;56:5594–9. [PubMed: 8971161]
31. McDonnell TJ, Troncoso P, Brisbay SM, Logothetis C, Chung LW, Hsieh JT, Tu SM, Campbell ML. Expression of the protooncogene bcl-2 in the prostate and its association with emergence of androgen-independent prostate cancer. Cancer Res 1992;52:6940–4. [PubMed: 1458483]
32. Navone NM, Troncoso P, Pisters LL, Goodrow TL, Palmer JL, Nichols WW, von Eschenbach AC, Conti CJ. p53 protein accumulation and gene mutation in the progression of human prostate carcinoma. J Natl Cancer Inst 1993;85:1657–69. [PubMed: 7692074]

33. Heidenberg HB, Sesterhenn IA, Gaddipati JP, Weghorst CM, Buzard GS, Moul JW, Srivastava S. Alteration of the tumor suppressor gene p53 in a high fraction of hormone refractory prostate cancer. J Urol 1995;154:414–21. [PubMed: 7609105]

34. Myers RB, Oelschlager D, Srivastava S, Grizzle WE. Accumulation of the p53 protein occurs more frequently in metastatic than in localized prostatic adenocarcinomas. Prostate 1994;25:243–8. [PubMed: 7971515]

35. Apakama I, Robinson MC, Walter NM, Charlton RG, Royds JA, Fuller CE, Neal DE, Hamdy FC. bcl-2 overexpression combined with p53 protein accumulation correlates with hormone-refractory prostate cancer. Br J Cancer 1996;74:1258–62. [PubMed: 8883414]

36. Bauer JJ, Sesterhenn IA, Mostofi FK, McLeod DG, Srivastava S, Moul JW. Elevated levels of apoptosis regulator proteins p53 and bcl-2 are independent prognostic biomarkers in surgically treated clinically localized prostate cancer. J Urol 1996;156:1511–6. [PubMed: 8808919]

37. Israels LG, Israels ED. Apoptosis. Oncologist 1999;4:332–9. [PubMed: 10476545]

38. Sordello S, Bertrand N, Plouet J. Vascular endothelial growth factor is up-regulated in vitro and in vivo by androgens. Biochem Biophys Res Commun 1998;251:287–90. [PubMed: 9790948]

39. Stewart RJ, Panigrahy D, Flynn E, Folkman J. Vascular endothelial growth factor expression and tumor angiogenesis are regulated by androgens in hormone responsive human prostate carcinoma: evidence for androgen dependent destabilization of vascular endothelial growth factor transcripts. J Urol 2001;165:688–93. [PubMed: 11176459]

40. Mazzucchelli R, Montironi R, Santinelli A, Lucarini G, Pugnaloni A, Biagini G. Vascular endothelial growth factor expression and capillary architecture in high-grade PIN and prostate cancer in untreated and androgen-ablated patients. Prostate 2000;45:72–9. [PubMed: 10960845]

41. Jain RK, Safabakhsh N, Sckell A, Chen Y, Jiang P, Benjamin L, Yuan F, Keshet E. Endothelial cell death, angiogenesis, and microvascular function after castration in an androgen-dependent tumor: role of vascular endothelial growth factor. Proc Natl Acad Sci USA 1998;95:10820–5. [PubMed: 9724788]

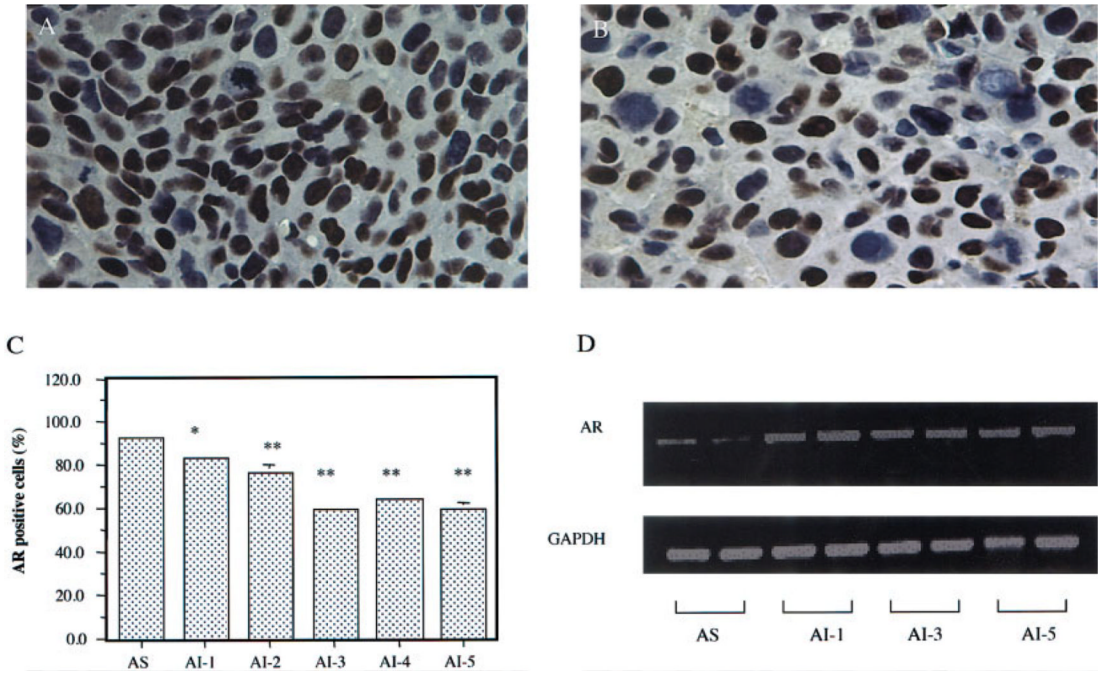

Figure 1.

Effects of androgen-independent (AI) tumor progression on androgen receptor (AR) expression. AR protein was immunohistochemically detected in the androgen-sensitive (AS) tumor *(a)* and in the androgen-independent (AI) tumor *(b)* (original magnification, ×400). AR-positive cells were stained brown. The percentages of AR-positive tumor cells were 92.6% in the AS tumor and were decreased from 83.3%to 59.2% in the AI-1 to AI-5 tumors *(c)*. Values with asterisks are significantly different from the AS control (*$p < 0.05$; **$p < 0.01$). RT-PCR analysis indicated that the AI tumors had increased expression of AR mRNA compared to the AS tumor *(d)*. Values are expressed as means ± SEM. For each generation, $n = 4$.

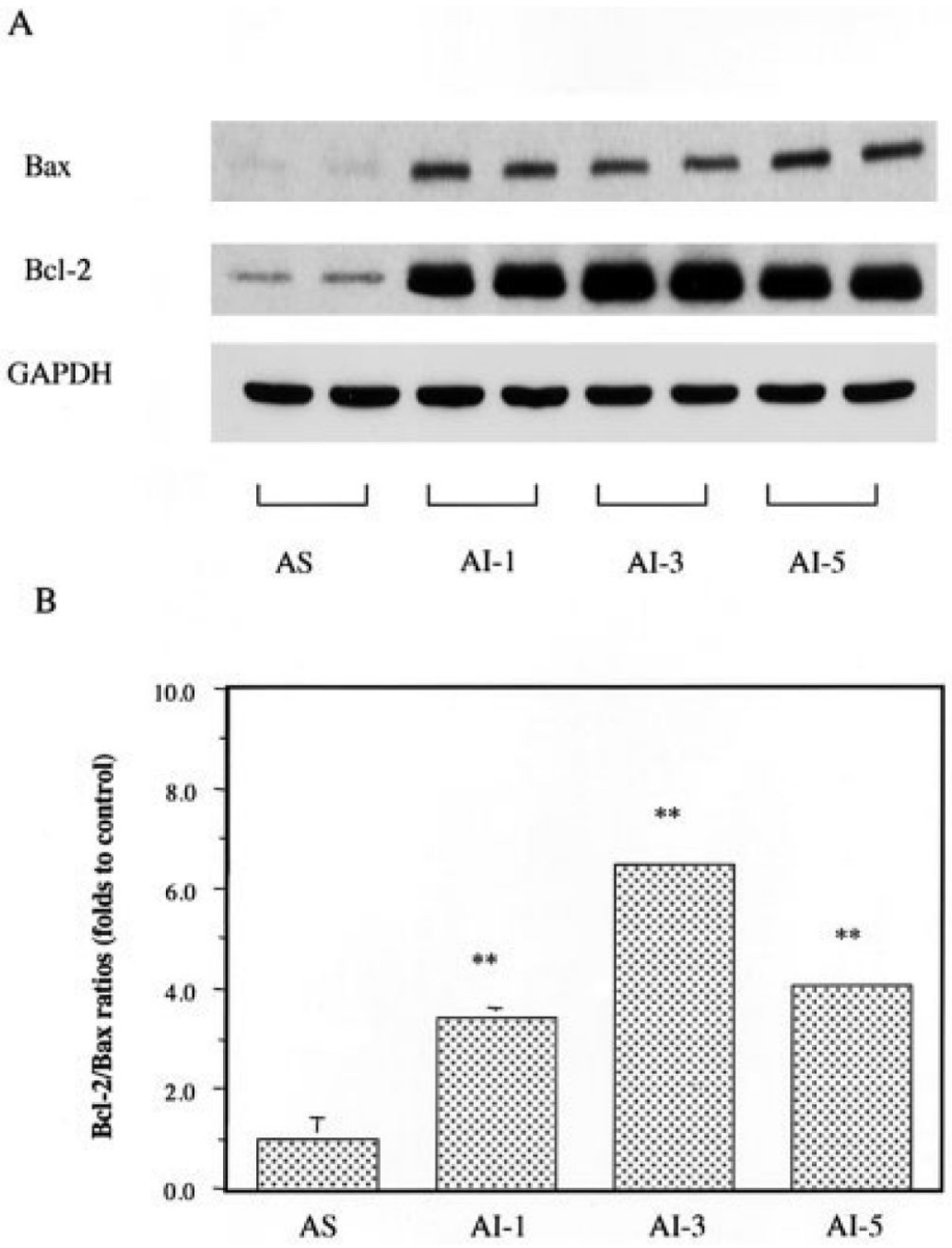

Figure 2.

Effects of androgen-independent (AI) tumor progression on the expression of bax and bcl-2 proteins. Both bcl-2 and bax proteins were significantly higher in the AI tumors than that in the androgen-sensitive (AS) tumors *(a)*. The increase of bcl-2 expression was higher than that of bax, resulting in significant 3-fold to 7-fold increases of bcl-2/Bax ratios in the AI tumors *(b)*. Values with asterisks are significantly different from the AS control (**$p < 0.01$). Values are expressed as means ± SEM.

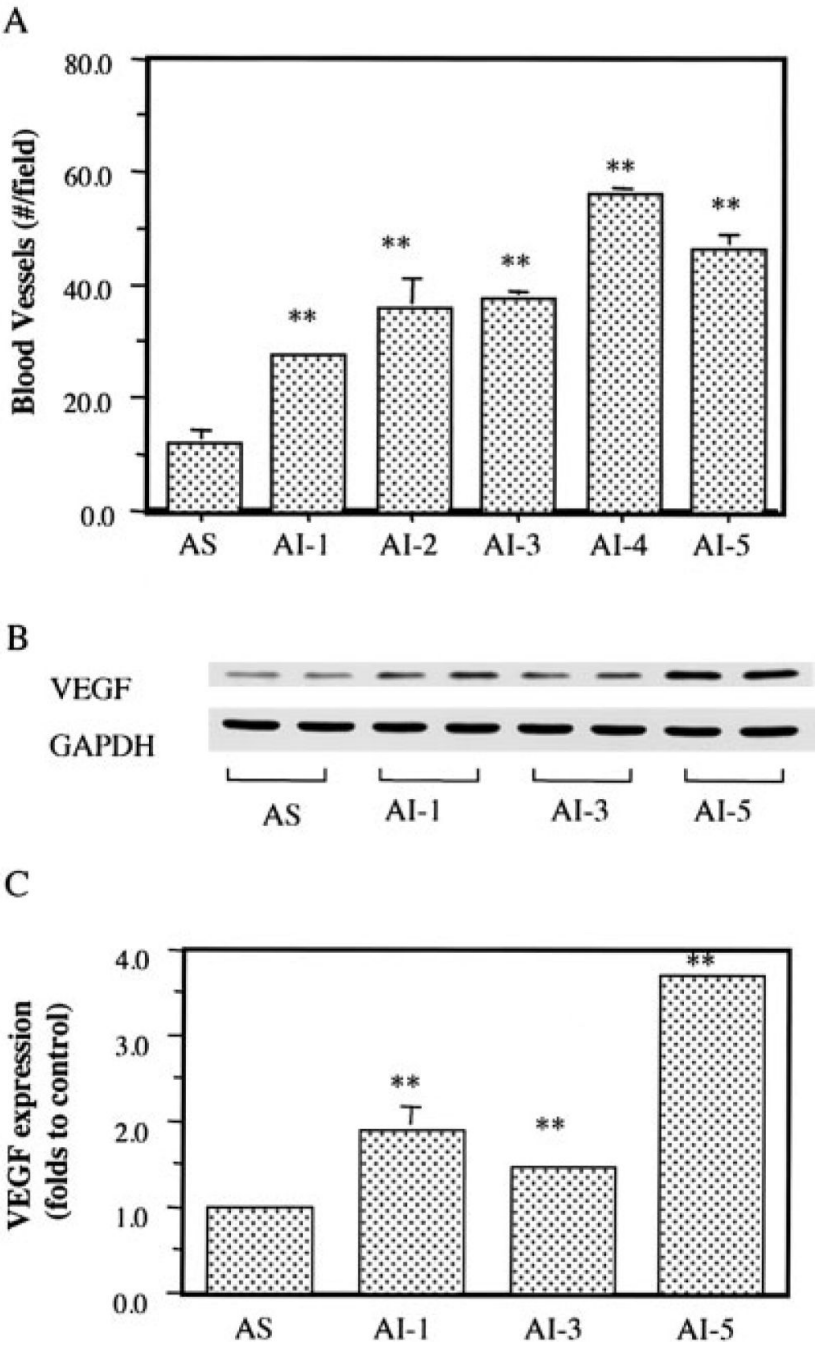

Figure 3.

Effects of androgen-independent (AI) tumor progression on blood vessel formation and VEGF expression. *(a)* Blood vessel numbers in the androgen-sensitive (AS) and AI tumors. *(b)* Western blot analysis of VEGF expression in the AS and AI tumors. *(c)* Quantification of VEGF expression. Values with asterisks are significantly different from the AS control (**$p < 0.01$).

TABLE I

EFFECTS OF AI TUMOR PROGRESSION ON TUMOR CELL PROLIFERATION, APOPTOSIS AND EXPRESSION OF P53 AND P21/WAF1

Treatment	Proliferation index (% total cells)	Apoptotic index (% total cells)	p53		p21/waf1	
			Positive cells (% total cells)	Intensity (% AS tumor)	Positive cells (% total cells)	Intensity (% AS tumor)
AS	16.4 ± 8.1	9.99 ± 0.75	6.8 ± 2.6	100.0	3.89 ± 1.19	100.0
AI-1	36.4 ± 2.5[1]	2.79 ± 0.78[2]	9.5 ± 0.6	130.5 ± 8.6[2]	15.97 ± 6.12[1]	154.3 ± 4.3[2]
AI-2	38.3 ± 4.0[1]	3.96 ± 0.17[2]	30.1 ± 5.8[2]	139.7 ± 1.4[2]	13.56 ± 2.60	165.0 ± 0.2[2]
AI-3	39.2 ± 5.2[1]	4.19 ± 0.25[2]	27.3 ± 1.6[2]	145.6 ± 2.1[2]	21.39 ± 0.97[2]	167.2 ± 0.4[2]
AI-4	36.5 ± 8.4[1]	2.84 ± 0.19[2]	28.1 ± 1.4[2]	153.0 ± 4.5[2]	18.46 ± 2.32[1]	168.9 ± 2.6[2]
AI-5	36.7 ± 1.4[1]	2.66 ± 0.75[2]	29.9 ± 0.5[2]	149.6 ± 7.0[2]	12.78 ± 2.54	165.8 ± 0.8[2]

Values are means ± SD.-AI, androgen-independent; AS, androgen-sensitive

[1]Value is significant from that of the AS tumor, $p < 0.05$

[2]Value is significant from that of the AS tumor, $p < 0.01$